RSC Advances

ROYAL SOCIETY OF CHEMISTRY

www.rsc.org/advances

The main contributions to the fundamental understanding of this paper are as follows.

1. In order to obtain hydrogen-bonded supramolecular polymer from amide groups, which is a common linkage for conventional polymers but suffers from low hydrogen-bonding strength for fabricating supramolecular polymers, a novel difunctional monomer, 1,12-di(2-pyridinecarbaldehyde-4'-hydrazinephenylate) dodecane (defined as DPCHP-DODE), was successfully designed and synthesized through a two-step reaction process.

2. Because the electron densities of both proton donor and proton acceptor were modulated by the substitutes, the amide groups could form stronger hydrogen-bonding interactions. The effect of electron density of proton donors and proton acceptors could be confirmed by comparing the dynamic mechanical properties at amorphous state between DPCHP-DODEcooled and quenched di(2-pyridine carbaldehyde)-hexanediohydrazide (DPCHcooled), a designed monomer with electron density modulation on proton donor only.

3. The samples formed after cooling the melt DPCHP-DODE demonstrated a series of properties similar to conventional polymers, including fibers dragged from the melt, adhere to glass substrate, glass-transition, board melting range, irreversible melting and crystallization process, and solid-like dynamic mechanical properties.

4. Hydrogen-bonding interactions between amide groups were further discussed based on temperature-dependent FT-IR spectra, and the formation mechanism for the supramolecular polymer was suggested.

5. This research not only provides the first example to achieve supramolecular polymer using amide groups as the bonding motif to the best of our knowledge, but also offers a way for fabricating novel supramolecular polymers by adjusting the substitute effect.

RSC Advances

Paper

Novel Supramolecular Polymer Fabricated via Stronger Hydrogen-Bonding Interactions between Substituted Amide Groups: Design, Synthesis, Properties and Mechanism

Ze-Hui Dai, Lu Qiang, Liming Tang*, Bao-Hua Guo

Received 00th January 20xx,
Accepted 00th January 20xx

DOI: 10.1039/x0xx00000x

www.rsc.org/

A novel difunctional monomer, 1,12-di(2-pyridine carbaldehyde-4'-hydrazinephenylate) dodecane (defined as **DPCHP-DODE**), was designed and synthesized through a two-step reaction process. The chemical structure of **DPCHP-DODE** was confirmed by ^{1}H nuclear magnetic resonance (^{1}H-NMR) spectrum, Fourier-transform infrared (FT-IR) spectrum and elemental analysis (EA). Because the electron densities of both proton donor (N-H) and proton acceptor (C=O) were modulated by the substitutes, amide groups could form stronger hydrogen-bonding interactions between them. With such substituted amide groups at both ends, the molecules of **DPCHP-DODE** assembled into supramolecular polymer during the cooling process of the melting **DPCHP-DODE**, and the resulting samples (defined as **DPCHP-DODE$_{110}$** for the isothermal crystallized sample) exhibited a series of properties similar to conventional polymers, such as fibers dragged from the melt, adhere to glass substrate, glass-transition, board melting range, irreversible melting and crystallization process, and solid-like dynamic mechanical properties. Especially, **DPCHP-DODE $_{110}$** could adhere to glass substrate with shear strength of 0.8 MPa, which is comparable to that of poly alpha-olefins/styrene-ethylene-butylene copolymer hot-melt adhesive (0.9 MPa-1.3 MPa). The effect of electron density of proton donors and proton acceptors could be confirmed by comparing the dynamic mechanical properties at amorphous state between **DPCHP-DODE$_{cooled}$** and quenched di(2-pyridine carbaldehyde)-hexanediohydrazide **(DPCH$_{cooled}$)**, a designed monomer with electron density modulation on proton donor only. Moreover, Temperature-dependent FT-IR spectra were used to identify the differences in supramolecular interactions between **DPCHP-DODE** and **DPCHP-DODE $_{110}$**. Although both hydrogen-bonded and free C=O and N-H groups existed in them, **DPCHP-DODE $_{110}$** had more hydrogen-bonded C=O and N-H groups both at room temperature and during the heating process, which might be responsible for the polymer properties. Based on which, the formation mechanism of the supramolecular polymer was finally suggested.

1 Introduction

Supramolecular polymers formed from low molecular weight components, or monomers, via highly directional and reversible non-covalent bonds, display a series of properties similar to conventional high molecular weight covalent polymers, such as elasticity and mechanical properties[1-3]. Supramolecular polymer system could be built up by one or several kinds of supramolecular interactions, such as hydrogen-bonds[4-10], metal-ligand interactions[11-14], and π-π stacking[15-17], ionic interactions[18,19], host-guest interactions[20-24], hydrophobic interactions[25,26] and charge transfer interactions[27]. Since the bond energies of these types of supramolecular interactions (8-80 kJ/mol) are weaker than those of covalent bonds, such as C-C bond (347 kJ/mol) and C-O bond (351 kJ/mol) in the backbone of conventional polymers[28], supramolecular polymers exhibit dynamic equilibriums among monomer, oligomer and supramolecular polymer[29]. Therefore supramolecular materials show properties which could be modulated by external stimuli such as heat[30,31], light[32,33], pH[34,35] and ions[36]. They also display potential applications in advanced technologies such as liquid crystal[37], photoelectric materials[38] and dielectric materials[39].

It has been known that the strength of the hydrogen-bonding interactions becomes stronger by varying the number and configuration of the hydrogen bonds in a particular array[40,41]. Therefore hydrogen-bonded supramolecular polymers are mostly formed via multiple hydrogen-bonding systems, for example guanine-cytosine triple hydrogen-bonding system[42] and 2-ureido-4-pyrimidone quadruple hydrogen bonding system[43,44]. However, multiple hydrogen-bonding systems often meet with some inherent shortcomings, such as lower reactivity, lower solubility in common solvents, complex chemical structure and complicated preparation procedure[1]. Therefore it is desired to develop simple and effective hydrogen-bonding motifs from practical view point.

The strength of the hydrogen-bonding interactions depends on not only the numbers of hydrogen-bonding arrays, but also the electrostatic interactions between the proton donors and

Key Laboratory of Advanced Materials of Ministry of Education of China, Department of Chemical Engineering, Tsinghua University, Beijing 100084.
E-mail: tanglm@tsinghua.edu.cn; Fax: +86-10-62770304; Tel: +86-10-62782148
† Electronic Supplementary Information (ESI) available. See DOI:10.1039/x0xx00000x

proton acceptors[45,46]. Therefore the strength of hydrogen-bonding interactions relies strongly on the electron densities of the donors and acceptors[47,48]. The higher electron density in the proton acceptor and the lower electron density in the proton donor, the stronger hydrogen-bonding interactions form. This unique feature should become a simple way to adjust hydrogen-bonding strength[48,49]. Amide groups, as the linkages of the backbones, have great influences on superstructures and properties of biopolymers and synthetic polymers, but have seldom been applied to fabricate supramolecular polymers because of their limited hydrogen-bonding strength. It is assumed that stronger hydrogen-bonding interactions might be achieved via modulating the substituents of amide groups.

To obtain hydrogen-bonded supramolecular polymer from amide groups, a novel difunctional monomer, 1,12-di(2-pyridinecarbaldehyde-4'-hydrazinephenylate) dodecane (defined as **DPCHP-DODE**, scheme 1) was designed and synthesized through a two-step reaction process. Because the electron densities of both proton donor and proton acceptor were modulated by the substitutes, the amide groups could form stronger hydrogen-bonding interactions between them. As a result, samples demonstrated a series of properties similar to conventional polymer materials after cooling the melt of **DPCHP-DODE**.

In this article, we designed a difunctional monomer **DPCHP-DODE** with two ended amide groups and tried to prepare it through a two-step reaction procedure. Then a series of supramolecular polymer properties were investigated for the samples formed after cooling the melting **DPCHP-DODE**, including fibers dragged from the melt, bonding to glass substrate, glass-transition, board melting range, irreversible melting and crystallization process, and solid-like dynamic mechanical properties. Finally, hydrogen-bonding interactions between amide groups were discussed in detail based on temperature-dependent FT-IR spectra, and the formation mechanism for the supramolecular polymer was suggested. To the best of our knowledge, this research provided the first example to achieve supramolecular polymer using amide groups as the bonding motif. The method to strengthen weak interactions via adjusting the substitute effect might be applied to many other hydrogen-bonding systems, which are helpful for fabricating novel supramolecular polymers.

2 Experimental Section

2.1 Materials

4-Hydroxybenzhydrazide, 2-pyridinecarboxaldehyde, 2-pyridinecarbaldehyde- 4'-hydroxybenzoyl hydrazine were all purchased from Sigma Aldrich. Adipic dihydrazide **(ADH)** was purchased from Weifang Chemidea Chemicals Co., LTD.,. Analytical solvents, including ethanol, N,N-dimethyl formamide (DMF) and dimethylsulfoxide (DMSO) were purchased from Beijing Chemical Works. All the materials and solvents were used directly without further purification.

2.2 Synthesis of monomer DPCHP-DODE

1,12-di(2-pyridinecarbaldehyde-4'-hydrazinephenylate) dodecane (**DPCHP-DODE**) was synthesized via a two-step reaction procedure as outlined in scheme 1.

Synthesis of 2-pyridinecarbaldehyde-4'-hydroxybenzoyl hydrazine (3)

The solution of 2-pyridinecarboxaldehyde (**2**) (3.00 g, 28.0 mmol) in ethanol (20 mL) was dropped into the suspension of 4-hydroxybenzhydrazide (**1**) (2.88 g, 18.9 mmol) with a drop of acetic acid in ethanol (50 mL) and the reaction was conducted at room temperature for 20 hrs. After filtration and dried in vacuum at 50 ºC for 10 hours to remove any residual solvent, white powder of 2-pyridinecarbaldehyde-4'-hydroxybenzoyl hydrazine (**3**) (3.60 g, in 78.9% yield) was obtained[50,51].

***Synthesis of Monomer* DPCHP-DODE**

2-pyridinecarbaldehyde-4'-hydroxybenzoyl hydrazine (**3**) (2.35 g, 9.75 mmol) was dissolved in DMF (30 mL) and then potassium carbonate (K_2CO_3) (1.35 g, 9.78 mmol) was added into the solution to form a suspension. The solution of 1,12-dibromododecane (**4**) (1.60 g, 4.88 mmol) in DMF (30 mL) was dropped into the former suspension. After that, the reaction proceeded at 60 ºC under stirring for 6 hrs. After filtration, the precipitate was recrystallized in DMSO for three times to give **DPCHP-DODE** (1.60 g , in 50.5% yield).

Monomer **DPCHP-DODE**, ^{1}H-NMR (DMSO-D6, 300 MHz, δ/ppm, Fig. 1): 1.26~1.40 (m, 16H, H atoms in the solid box, k), 1.71 (m, 4H, j), 4.02 (t, 4H, i), 7.03 (d, 4H, a), 7.38 (t, 2H, g), 7.88 (d, 4H, b), 7.94 (m, 4H, e and f), 8.44 (s, 2H, d), 8.58 (d, 2H, h), 11.87 (s, 2H, c). J_{ab}=9.0 Hz, J_{gh}=4.5 Hz, J_{ij}=6.3 Hz, J_{jk}=6.0 Hz. FT-IR spectroscopy (KBr, cm^{-1}, Fig. S2): 3246 cm^{-1} and 3216 cm^{-1} (N-H), 3072 cm^{-1}, 3050 cm^{-1} and 3010 cm^{-1} (C-H in aromatic group), 2916 cm^{-1} and 2850 cm^{-1} (C-H in alkyl chain), 1679 cm^{-1} and 1652 cm^{-1} (amide I group), 1543 cm^{-1} (amide II group). EA, $C_{38}H_{44}N_6O_4$, theoretical value: C 70.35%, H 6.84%, N 12.95%, O 9.86%; experimental data: C 70.36%, H 6.83%, N 12.95%, O 9.86%.

2.3 Sample preparation

The sample of **DPCHP-DODE$_{cooled}$** was prepared by cooling the melt of M from 210 ºC to 30 ºC at a cooling rate of 10 ºC/min on a Linkam LTS420 hot-stage. The samples of **DPCHP-DODE$_{110}$**, **DPCHP-DODE$_{115}$** and **DPCHP-DODE$_{120}$** were prepared by isothermal crystallization of the melt of M at 110 ºC, 115 ºC and 120 ºC after melting at 210 ºC for 3 min, respectively.

2.4 Methods

The molecular structure of **DPCHP-DODE** was determined by ^{1}H-NMR spectrometer (JEOL, ECA-300M) with DMSO-D6 as a solvent and tetramethylsilane as a reference.

The shear strength of the bonded lap joints was measured by a universal tensile machine (UTM-1432, Chengde Jinjian). Lap joints bonded with **DPCHP-DODE$_{110}$** between two glass substrates were prepared by isothermal crystallization of the **DPCHP-DODE** melt at 110 ºC after melting at 210 ºC for 3 min. The reported shear strength is the average of three measurements.

The heat properties of **DPCHP-DODE**, **DPCHP-DODE$_{cooled}$** and **DPCHP-DODE$_{110}$** were studied by a differential scanning calorimeter (DSC, TA-2000) equipped with intercooler as cooling

system under an atmosphere of nitrogen.

Dynamic mechanical properties were carried out on an Anton Paar Physica MCR301 Rheometer equipped with parallel plate (diameter 25 mm). The strain in the oscillatory was set as 0.05% for the frequency and temperature scanning. For temperature scanning, the frequency was 1 Hz and the heating rate was 4 ºC/min. For frequency scanning of **DPCHP-DODE$_{cooled}$** in the range of 0.01 Hz to 100 Hz, the temperature was set at 50 ºC after melting at 205 ºC. The storage modulus (*G*'), loss modulus (*G*") and damping factor (tanδ) were measured.

The morphologies of **DPCHP-DODE$_{110}$**, **DPCHP-DODE$_{115}$** and **DPCHP-DODE$_{120}$** samples were observed by a polarizing microscope (POM, Olympus BX41P) equipped with a Linkam LTS420 hot-stage.

Fourier transform infrared spectrometry (FT-IR) studies were performed on a Nicolet-560 IR spectrometer at a resolution of 4 cm^{-1} in the wavenumber range of 4000-400 cm^{-1} over 32 scans.

Thermogravimetric analysis (TGA) of **DPCHP-DODE** and **DPCHP-DODE$_{110}$** were carried out on a TGA analyzer (TA, Q5000-IR) from ambient temperature to 900 ºC in nitrogen.

3 Results and discussion

3.1 Design and structure of Monomer DPCHP-DODE

In order to form supramolecular polymer with hydrogen-bonding interactions between amide groups, a novel monomer with substituted amide groups at both ends, 1,12-di(2-pyridine carbaldehyde-4'-hydrazinephenylate)dodecane (**DPCHP-DODE**) was prepared through a two-step reaction procedure as indicated in Scheme 1. Firstly, the dehydration reaction between 4-hydroxybenzhydrazide (**1**) and 2-pyridinecarboxaldehyde (**2**) gave 2-pyridinecarbaldehyde-4'-hydroxybenzoyl hydrazine (**3**) in 78.9% yield. Then **DPCHP-DODE** was synthesized in 50.5% yield by the substitution reaction between (**3**) and 1,12-dibromododecane (**4**).

The chemical structure of **DPCHP-DODE** was confirmed by ^{1}H-NMR (**Fig. 1**), FT-IR spectrum (**Fig. S1**) and EA (see the experimental section). All the results reveal that the chemical structure of the product is consistent with the design.

Normally, amide groups form weak hydrogen-bonding interactions with each other. The weak interactions could become stronger via adjusting the electronic environments of amide groups. In the chemical structure of **DPCHP-DODE**, the alkoxy group at the para-position of benzoyl amide has an electron donating effect on carbonyl group, leading to an increase of electron density in the proton acceptor (C=O)[52]. Attaching to both carbonyl group and the π-π conjugative system of pyridine group and C=N group, the p-π conjugative effects lowering the electron density of amine group as proton donor (N-H) obviously[49], thus leading to stronger electrostatic interaction between the proton donor and the proton acceptor. Therefore the amide groups in **DPCHP-DODE** could form stronger hydrogen-bonding interactions with themselves. Similar to conventional monomers with two reactive sites, **DPCHP-DODE** has two substituted amide groups at both ends and therefore the monomers are able to interlink together into extended architecture.

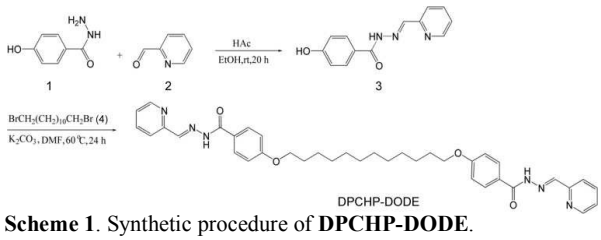

Scheme 1. Synthetic procedure of **DPCHP-DODE**.

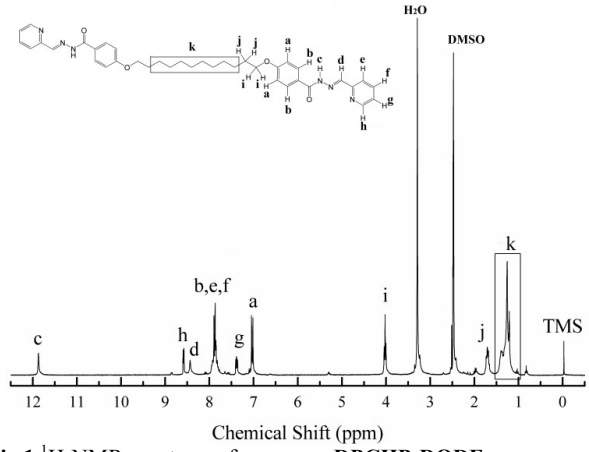

Fig.1 ^{1}H-NMR spectrum of monomer **DPCHP-DODE**.

3.2 Properties of supramolecular polymer

Based on the above analysis, **DPCHP-DODE** is assumed to form supramolecular polymer based on the stronger hydrogen-bonding interactions between amide groups. The supramolecular performances of the samples formed after cooling the melting **DPCHP-DODE** were investigated in detail.

We found that supramolecular fibers could form in the isothermal process with a large supercooling after the melting of **DPCHP-DODE**. In detail, **DPCHP-DODE** was cooled at 110 ºC after melting fully at 210 ºC. Fibers with a length of several centimeters could be drawn from the melt between two glass plates after keeping at 110 ºC for 30 s, as shown in Fig.2a. This should be due to a proper elasticity for the forming of long fibers and a proper viscosity for the drawing operation under such a large supercooling. Fibers could be drawn for many times after a repeated melting and cooling process of **DPCHP-DODE**.

Strong adhesion effect of cooled **DPCHP-DODE** on two glass substrates was also observed by prolonging the cooling time. Bonded lap joints with cooled **DPCHP-DODE** at 110 ºC (defined as **DPCHP-DODE$_{110}$**) exhibited considerable adhesion strength, as indicated in Fig.2b. The adhesive properties of the bonded lap joints were quantitatively measured by shear tests[53], which revealed shear strength of 0.82 MPa, as indicated in Fig.S3a. This is comparable to that of poly alpha-olefins/styrene-ethylene-butylene copolymer hot-melt adhesive (0.9 MPa-1.3 MPa)[54], which demonstrated strong shear strength for **DPCHP-DODE$_{110}$**. The shear tests also revealed cohesive failure for **DPCHP-DODE$_{110}$**, as shown in Fig.S3b, which indicated strong adhere ability to the glass substrate.

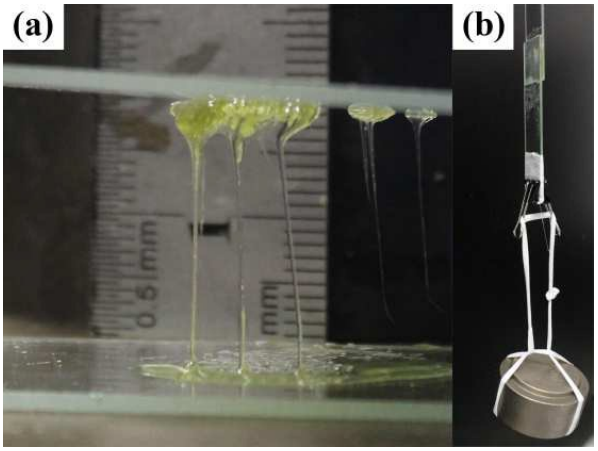

Fig.2 (a) Fiber formed from the melting **DPCHP-DODE** cooled at 110 ºC for 30 s; and (b) regular glasses bonded with **DPCHP-DODE$_{110}$** holding a weight of 200 g.

Such proper viscosity and elasticity properties under large supercooling, as well as the adhesion effects are not the features of conventional small molecular weight molecules, but are the features of some conventional polymers. Therefore, the formation of supramolecular fibers and the strong adhesion effect of **DPCHP-DODE$_{110}$** on glass substrates confirm the formation of supramolecular polymer.

Since **DPCHP-DODE** exhibits unusual viscosity and adhesion properties under such large supercooling, DSC was employed to study the thermal behaviors in the melting and cooling processes of **DPCHP-DODE**, as indicated in Fig.3, Fig.S4 and Table 1. Only one narrow but sharp peak is observed at T_m=195.0 ºC in the first heating process of **DPCHP-DODE** (**Fig.3a**). The melting range of the peak is 193.0-196.2 ºC, which coincides to the melting points observed by optical microscopy (OM). This sharp but narrow melting peak is typical for small molecular weight materials. However, no crystallization peak is observed in the subsequent cooling process during which **DPCHP-DODE$_{cooled}$** is prepared, revealing the irreversible melting and crystallization behaviors of monomer **DPCHP-DODE**.

Interestingly, some differences are observed in the further heating process of **DPCHP-DODE$_{cooled}$**, as indicated in **Fig.3b**. Firstly, a sudden change in heat capacity, or a glass transition process, appears at 60.0 ºC for **DPCHP-DODE$_{cooled}$**. This glass transition does not appear in the temperature range of 0~200 ºC for **DPCHP-DODE**. A glass-transition process is also observed for **DPCHP-DODE$_{110}$**, as shown in **Fig.3c**, even though with a decreased T_g compared to **DPCHP-DODE$_{cooled}$**, which indicating an increase of mobility in the amorphous phase[55]. Secondly, a cold crystallization peak (T_{cc}) is observed at 120.0 ºC for **DPCHP-DODE$_{cooled}$**, which is similar to the heating curve of conventional polymer with lower crystallinity. However, this cold crystallization behavior does not appear in **DPCHP-DODE$_{110}$**, as shown in **Fig.3c**, since **DPCHP-DODE$_{110}$** crystallized enough during the isothermal crystallization process at 110 ºC. Thirdly, different melting behaviors are observed for **DPCHP-DODE$_{cooled}$** compared with **DPCHP-DODE**. The melting temperature decreases to 184.4 ºC and 187.0 ºC, and a broader melting range of 178.6 ~189.6 ºC is observed for **DPCHP-DODE$_{cooled}$**. The glass transition, the cold crystallization peak, and the boarder melting peak in the heating process indicate that **DPCHP-DODE$_{cooled}$** show a series of thermal properties similar to conventional polymer materials.

In order to get a quantitative comparison in the mechanical properties of supramolecular polymers with different electron densities of proton donors and acceptors, dynamic mechanical properties of **DPCHP-DODE$_{cooled}$** and quenched (di(2-pyridine carbaldehyde)-hexanediohydrazide) (defined as **DPCH$_{cooled}$**), another supramolecular polymer formed by quenching the melt of monomer **DPCH**, were measured at 50 ºC in the frequency ranged from 10^{-1} Hz to 10^{2} Hz. The experimental section for synthesizing **DPCH** and ^{1}H-NMR spectrum is shown in Scheme S1 and Fig.S1 in the supporting information. Both **DPCHP-DODE$_{cooled}$** and **DPCH$_{cooled}$** show solid-like behaviours with G' about an order higher than G'', and they both have a damping factor less than 1, which are attribute to the formation of network structure in the glassy state of **DPCHP-DODE$_{cooled}$** and **DPCH$_{cooled}$**[5], as indicated in Fig.4a and Fig.S5. More importantly, both G' and G'' of **DPCHP-DODE$_{cooled}$** are about 1 order higher than those of **DPCH$_{cooled}$**. Both **DPCH$_{cooled}$** and **DPCHP-DODE$_{cooled}$** are amorphous materials, as the cooling process indicated in Fig S4a and Fig S6. The structure of **DPCH** was designed based on the principle that only the proton

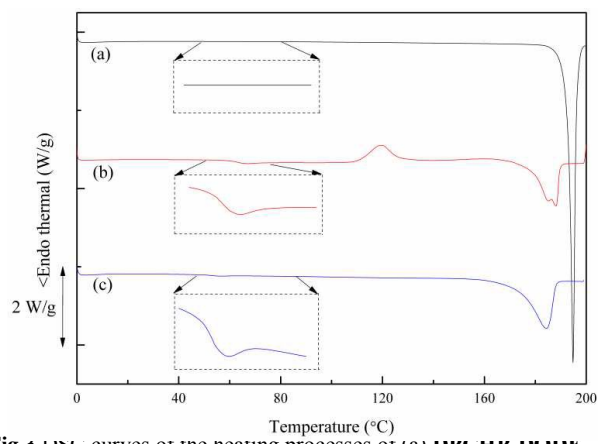

Fig.3 DSC curves of the heating processes of (a) **DPCHP-DODE**, (b) **DPCHP-DODE$_{cooled}$**, and (c) **DPCHP-DODE$_{110}$**.

Table 1 Thermal properties in the heating processes of **DPCHP-DODE**, **DPCHP-DODE$_{cooled}$** and **DPCHP-DODE$_{110}$**

Sample	T_g (ºC)	T_{cc} (ºC)	T_m (ºC)				ΔH_m (J/g)
			onset	peak1	Peak2	endset	
DPCHP-DODE	-	-	193.0	195.0	-	196.2	-114.7
DPCHP-DODE$_{cooled}$	60.0	120.0	178.6	184.4	187.0	189.6	-74.6
DPCHP-DODE$_{110}$	51.0	-	174.0	184.4	-	188.4	-75.8

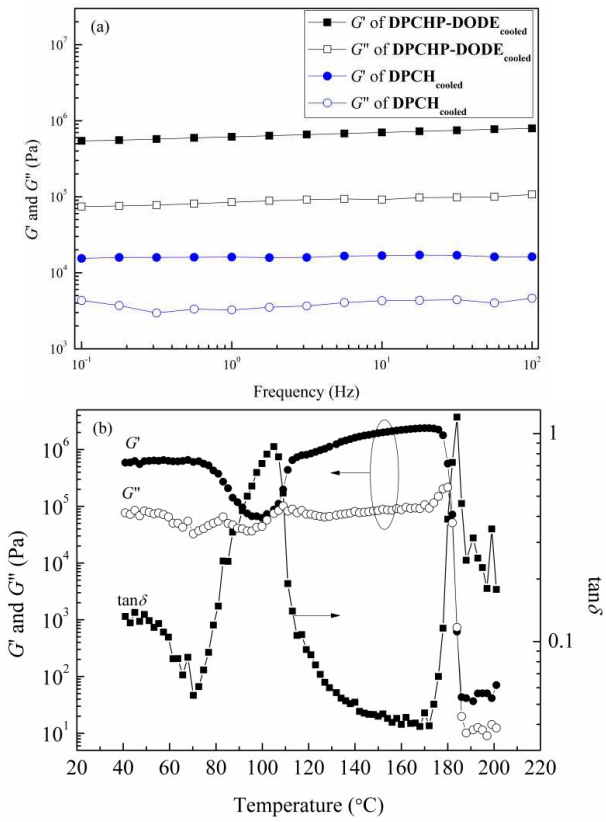

Fig.4 (a) Storage modulus (*G*'), loss modulus (*G*") of **DPCHP-DODE$_{cooled}$** and **DPCH$_{cooled}$** at frequency ranged between 0.1 Hz and 100 Hz at 50 ºC and (b) at temperature scanning ranged between 40 ºC and 200 ºC of **DPCHP-DODE$_{cooled}$** at a frequency of 1 Hz.

donor, i.e. the amide group, is modulated by attaching it to π-π conjugative system of pyridine group and C=N group. Similar to monomer **DPCHP-DODE**, the electron density of the proton donor is lowered by p-π conjugative effects. However, the electron densities of proton donor and proton acceptor were both modulated by the substitute groups of the amide group in **DPCHP-DODE**. Therefore, the difference in *G*' and *G*" between the amorphous **DPCHP-DODE$_{cooled}$** and **DPCH$_{cooled}$** might be due to the strength of the hydrogen-bonding interactions. Stronger hydrogen-bonding interactions formed in **DPCHP-DODE$_{cooled}$** with electron density modulation on both proton donor and proton acceptor, therefore results in higher *G*' and *G*" of **DPCHP-DODE$_{cooled}$**.

For temperature scanning in the heating process of **DPCHP-DODE$_{cooled}$**, as indicated in Fig.4b, higher *G*' compared to *G*" and a damping factor less than 1 are observed at all temperature before the melting of **DPCHP-DODE$_{cooled}$**. Moreover, a strong peak in the tan*δ* curve is observed at the temperature range between 80 ºC and 110 ºC, while two peaks are observed in this temperature range in the curve of *G*". According to the DSC results of **DPCHP-DODE$_{cooled}$**, the two peaks at 80 ºC and 105 ºC in the *G*" curve could be assigned to the glass transition and cold crystallization, respectively. The large asymmetric peak in the tan*δ* curve is assigned to the sum of the aforementioned two phase transition processes. The variance in the *G*' curve at this temperature range could also be attributed to the two phase transitions. The decrease of *G*' is assigned to the glass-transition since material in its rubbery state exhibits lower modulus compared with that in its glassy state, while the increase of *G*' at higher temperatures is assigned to cold crystallization since material in its crystalline phase exhibits higher modulus compared with that in its amorphous phase. A sudden decrease of *G*' and *G*" and a peak of tan*δ* at around 180 ºC (Fig.4b) are attributed to the melting of **DPCHP-DODE$_{cooled}$** according to the DSC results. However, *G*' is still larger than *G*" at above 180 ºC, which might be due to the existence of some residual network structure formed of weak intermolecular interactions.

The morphologies of **DPCHP-DODE$_{110}$**, **DPCHP-DODE$_{115}$** and **DPCHP-DODE$_{120}$** were further observed by a polarized optical microscopy with a compensating plate at 530 nm, as indicated in Fig.5. It is clear that the nucleation density highly depends on supercooling. The nucleation density increases with the decreasing the crystallization temperature, which is 60~70 ºC lower than the melting peak of M (Fig.5a, Fig.5b, Fig.5c). Fibrous structure appears around the nuclei at the initial stage, which gradually branches off and fills the whole area (Fig.5d). These fibers show strong anisotropy effect. Blue fibers appear in the first and the third quadrant, while yellow fibers appear in the second and the fourth quadrant, indicating stronger effect in the fiber direction than in the tangential direction.

3.3 Investigation of hydrogen-bonding interactions by FT-IR

From the above results, **DPCHP-DODE$_{cooled}$** and **DPCHP-DODE$_{110}$** display a series of properties similar to conventional polymers. To understand the major differences in FT-IR spectra of **DPCHP-DODE** and **DPCHP-DODE$_{110}$** are presented in Fig.6. The absorption bands at the range between 3300 and 3100 cm^{-1} are assigned to the stretching modes of N-H, while the absorption bands at the range of 3100-3000 cm^{-1} are assigned to the stretching mode of unsaturated C-H in aromatic rings (Fig.6a). Compared to **DPCHP-DODE**, **DPCHP-DODE$_{110}$** shows quite different absorption at the same range between 3300 and 3100 cm^{-1}. At the range between 1725 and 1625 cm^{-1}, some other differences are also observed for the two samples, which should be assigned to the amide I band consisting of the stretching modes of C=O and C-N groups (Fig.6b).

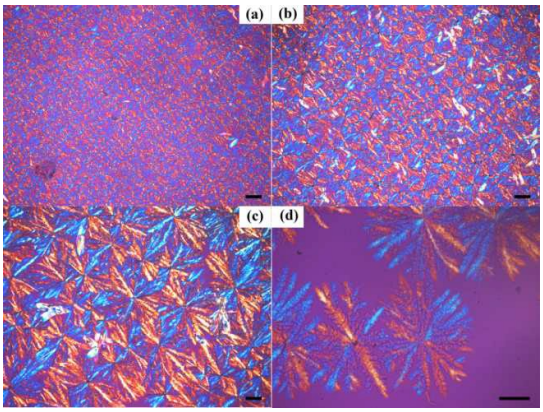

Fig.5 POM images of **DPCHP-DODE** isothermal crystallized at (a) 110 ºC, (b) 115 ºC, (c) 120 ºC and (d) initial image at 120 ºC. (All scale bar is 50 μm)

In order to further identify the differences between M and M_{110}, peak fit of these N-H and C=O absorption peaks was carried out, as shown in Fig.6. For the N-H stretching band, two absorption peaks at 3216 cm^{-1} and 3246 cm^{-1} are observed in **DPCHP-DODE** with their peak area ratio of 1.15 ($A_{3216/3246}$). While for **DPCHP-DODE$_{110}$**, the two absorption peaks at 3200 cm^{-1} and 3247 cm^{-1} display a peak area ratio of 2.45 ($A_{3200/3247}$). The two absorption peaks might demonstrate the existence of two types of N-H in both **DPCHP-DODE** and **DPCHP-DODE$_{110}$**. According to the experimental facts that the band at 3216 cm^{-1} (in **DPCHP-DODE**) red-shifts to 3200 cm^{-1} (in **DPCHP-DODE$_{110}$**), while the bands at 3246 cm^{-1} (in **DPCHP-DODE**) and 3247 cm^{-1} (in **DPCHP-DODE$_{110}$**) exhibit no clear difference, it is assumed that the bands at 3200 cm^{-1} (in **DPCHP-DODE$_{110}$**) and 3216 cm^{-1} (in **DPCHP-DODE**) are assigned to hydrogen-bonded N-H, while the bands at 3246 cm^{-1} (in **DPCHP-DODE**) and 3247 cm^{-1} (in **DPCHP-DODE$_{110}$**) are assigned to free N-H. This assumption is in accordance with the literature results[56-58]. The increased peak area ratio (hydrogen-bonded N-H/free N-H) value in **DPCHP-DODE$_{110}$** compared to that in **DPCHP-DODE** indicates an increased amount of hydrogen-bonded N-H, which develops a boarder absorption band for N-H in **DPCHP-DODE$_{110}$**.

The differences in the absorption band of C=O in amide I group between **DPCHP-DODE** and **DPCHP-DODE$_{110}$** could also be noticed by the similar fit peak method, as revealed in Fig.6b. The two absorption peaks at 1679 cm^{-1} and 1652 cm^{-1} has a peak area ratio of 0.39 ($A_{1679/1652}$) for **DPCHP-DODE**, while they appear at 1681 cm^{-1} and 1650 cm^{-1} with their peak area ratio of 1.26 ($A_{1681/1650}$) for **DPCHP-DODE$_{110}$**. These results demonstrate that C=O in amide I group also consists of two types of C=O[56-58]. Similar to the blue shift of peak wavenumber in hydrogen bonded carbonyl groups with amino groups compared with free carbonyl groups according to the literatures[59], it could also be speculated that the absorption peak at 1680 cm^{-1} is assigned to hydrogen-bonded C=O, while the absorption bond at 1652 cm^{-1} is for free C=O. The increased peak area ratio (hydrogen-bonded C=O/free C=O) value in **DPCHP-DODE$_{110}$** compared to that in **DPCHP-DODE** indicates an increased amount of hydrogen-bonded C=O and finally develops a broader absorption peak in **DPCHP-DODE$_{110}$**.

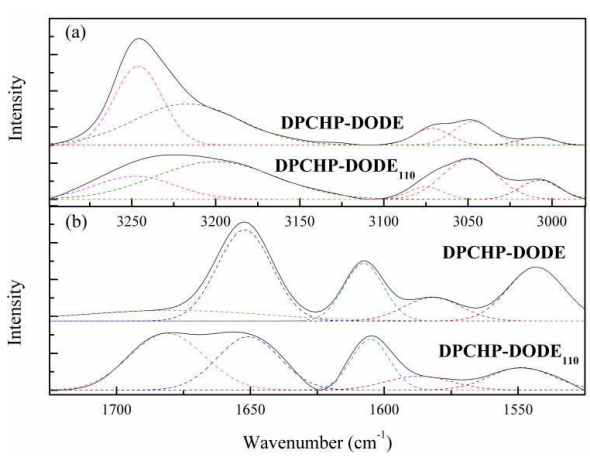

Fig.6 FTIR spectra of **DPCHP-DODE** and **DPCHP-DODE**$_{110}$ ranged (a) from 3300 to 2980 cm^{-1} and (b) from 1725 to 1525 cm^{-1}.

To further confirm our assumption on the hydrogen-bonded interactions, the temperature-dependent FT-IR in the heating process was carried out for **DPCHP-DODE** and **DPCHP-DODE$_{110}$** and the results are shown in Fig.S7. For **DPCHP-DODE**, the absorption areas at the bands of 3246 cm^{-1}, 3216 cm^{-1} and 1652 cm^{-1} decrease as increasing the temperature before melting, while no obvious change is observed for the band absorption area at the band of 1679 cm^{-1}, as revealed in Fig.S7a and Fig.S7b. For **DPCHP-DODE$_{110}$**, the peak areas at 3247 cm^{-1} and 1650 cm^{-1} increase, while the peak areas at 3200 cm^{-1} and 1681 cm^{-1} decrease as increasing the temperature, as revealed in Fig.S7c and Fig.S7d.

In order to eliminate the absorption coefficient difference caused by increasing temperature, the peak area ratio of N-H ($A_{3216/3246}$) and C=O ($A_{1679/1652}$) is used for the discussion of hydrogen-bonding interactions in the heating process, as shown in Fig.7. For **DPCHP-DODE**, the peak area ratio of C=O ($A_{1679/1652}$) remains unchanged while a slight decrease appears in the peak area ratio of N-H ($A_{3216/3246}$). However, for **DPCHP-DODE$_{110}$**, a sudden decrease of peak area is observed at above 100 ºC for C=O ($A_{1681/1650}$) and N-H ($A_{3200/3247}$). It is well-known that hydrogen-bonds dislocate gradually with increasing temperature, which will finally leads to a decrease of absorption bands area. Therefore, the absorption bands at 3200 cm^{-1} and 1681 cm^{-1} are assigned to the hydrogen bonded N-H and C=O, while the bands at 3247 cm^{-1} and 1650 cm^{-1} are assigned to the free N-H and C=O, respectively. These results are in accordance with the assumption mentioned above. As a result, the above mentioned peak area ratio, i.e. C=O ($A_{1679/1652}$) and N-H ($A_{3216/3246}$) for **DPCHP-DODE**, while C=O ($A_{1681/1650}$) and N-H ($A_{3200/3247}$) for **DPCHP-DODE$_{110}$**, are all belonging to the peak area ratio of hydrogen bonded groups/free groups.

Since larger peak area ratio of C=O ($A_{1679/1652}$) and N-H ($A_{3216/3246}$) are observed in **DPCHP-DODE$_{110}$** compared to that in **DPCHP-DODE** both at room temperature and in the heating process, as indicated in Fig.7, it could be speculated that there are more hydrogen-bonded N-H and C=O in **DPCHP-DODE$_{110}$** Therefore a possible formation mechanism of supramolecular polymer is suggested. Because each molecule of **DPCHP-DODE** has two amide groups, during the isothermal crystallization process, the molecules have high moving ability and they could form hydrogen-bonding interactions based on amide groups. As the monomer finally interlinked together via long-range hydrogen-bonding interactions, supramolecular polymer is formed. This might be responsible for the exhibition of supramolecular polymer properties of **DPCHP-DODE$_{110}$** which is prepared in isothermal crystallization process from the melting **DPCHP-DODE**. However, only a small amount of hydrogen-bonding interactions exists in **DPCHP-DODE** which is obtained by solution precipitation method. In such case, long-range hydrogen-bonding interactions could not form and therefore the sample lacks supramolecular properties. Our result provides direct evidence that supramolecular polymer properties could be developed based on hydrogen-bonding interactions between amide groups.

Both **DPCHP-DODE** and **DPCHP-DODE$_{110}$** display similar absorption bands when the measuring temperature was further elevated to 220 ºC as indicated in Fig.S8, which is much higher than the melting temperature. This result demonstrates that the hydrogen-

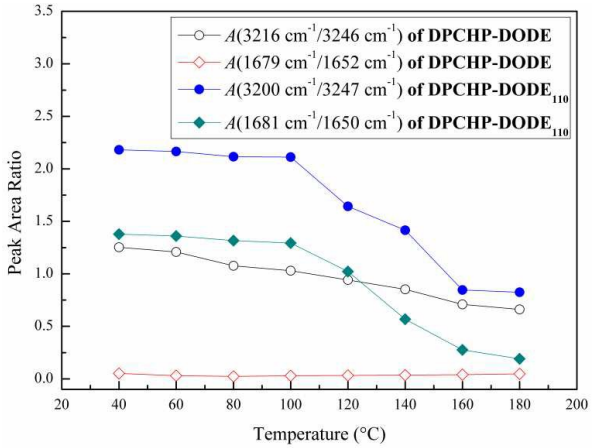

Fig.7 Plot of the peak area ratio of hydrogen-bonded and free N-H or C=O group in **DPCHP-DODE** and **DPCHP-DODE$_{110}$**.

bonding interactions are almost the same at that temperature, which leads to a similar thermal stability between **DPCHP-DODE** and **DPCHP-DODE$_{110}$**. At weight loss of 5%, the difference in the temperature between **DPCHP-DODE** and **DPCHP-DODE$_{110}$** is only 6 ºC, as indicated in Fig.S9.

The FT-IR spectra of **DPCHP-DODE** in the cooling process were also measured. The peak area ratio in the cooling process is hard to calculate since the existence of the broad amorphous peak of the melt **DPCHP-DODE**, as the FT-IR spectra of **DPCHP-DODE** in KBr in the cooling process shown in Fig. S10. Furthermore, As indicated in Fig.S11, the absorption peaks of C=O and N-H of the sample cooled from the melt in KBr sheet at 40 ºC (defined as **DPCHP-DODE$_{40\ in\ KBr}$**) are different from both **DPCHP-DODE** and **DPCHP-DODE$_{110}$**. The peak area ratio of **DPCHP-DODE$_{40\ in\ KBr}$** is 1.50 for $A_{3234/3257}$ and 0.451 for $A_{1677/1655}$. Both of these two peak area ratios are higher than those of **DPCHP-DODE** but lower than those of **DPCHP-DODE$_{110}$**. This indicates that the density of hydrogen-bonding interactions of **DPCHP-DODE$_{40\ in\ KBr}$** is higher than that of **DPCHP-DODE** monomer but lower than that of **DPCHP-DODE$_{110}$** and confirms that the hydrogen-bonding interactions do form in the cooling process of melt **DPCHP-DODE**. The lower hydrogen-bonding density may be due to the dilute effect of KBr as a medium for FT-IR measurements.

Based on temperature-dependent FT-IR investigations, it could be concluded that both hydrogen-bonded and free C=O groups and N-H groups coexist in monomer **DPCHP-DODE** and **DPCHP-DODE$_{110}$**. However, the difference in the ratio between hydrogen-bonded and free groups between **DPCHP-DODE** and **DPCHP-DODE$_{110}$** is observed at room temperature and in the heating process. The larger amount of hydrogen-bonding interactions in **DPCHP-DODE$_{110}$** is therefore responsible for long-range intermolecular interactions. Besides hydrogen-bonding interactions, we think some other supramolecular interactions may be responsible for the formation of supramolecular polymer, such as the π-π stacking of the aromatic groups, the micro-phase separation between polar hydrogen-bonding motifs and the apolar alkyl chains, and the entanglement of the flexible alkyl chains, all of which are now under investigation in our group.

In summary, novel monomer **DPCHP-DODE** with substituted amide groups at both ends of the molecule was prepared. The electron densities of both proton donor and proton acceptor were modulated by the substituent effects so as to form stronger hydrogen-bonding interactions. Based on which, supramolecular polymer with properties similar to ordinary polymers could be obtained via cooling the melt of **DPCHP-DODE**. The formation of hydrogen-bonding interactions was further confirmed by FT-IR analysis. Our research provides direct evidence that supramolecular polymer could be developed by modulating hydrogen-bonding interactions of amide groups. We believed that some other stronger hydrogen-bonding interactions could be designed from simple hydrogen bonding systems via modulating the electron densities of the donors and acceptors. The strategy in adjusting hydrogen-bonding strength might be helpful for constructing novel supramolecular polymers, especially from simple hydrogen-bonding systems.

4 Conclusion

A difunctional monomer, 1,12-di(2-pyridine carbaldehyde-4'-hydrazinephenylate) dodecane (**DPCHP-DODE**) with two 2-pyridine carbaldehyde-4'-hydroxybenzoyl hydrazine groups at both ends, was designed and synthesized through a two-step reaction process. By the substitute effects, the decrease of electron density in the proton donor and increase of electron density in the proton acceptor were accomplished, therefore leading to stronger hydrogen-bonding interactions between amide groups. The cooled samples of **DPCHP-DODE** melt exhibited a series of supramolecular properties similar to some conventional polymers, including fibers drawn from the supercooled melt, the strong adhesion to glass substrate, the glass transition, broader melting range compared to monomer **DPCHP-DODE**, irreversible melting and crystallization behaviors, and solid-state dynamic mechanical properties. The effect of electron density of proton donors and proton acceptors could be confirmed by comparing the dynamic mechanical properties at amorphous state between **DPCHP-DODE$_{cooled}$** and quenched di(2-pyridine carbaldehyde)-hexanediohydrazide (**DPCH$_{cooled}$**), a designed monomer with electron density modulation on proton donor only. Temperature-dependent FT-IR spectra were further used to identify the differences in the supramolecular interactions between **DPCHP-DODE** and **DPCHP-DODE$_{110}$**. It has been found that both hydrogen-bonded C=O and N-H, and free C=O and N-H coexisted in them. However, there are more hydrogen-bonded C=O and N-H in **DPCHP-DODE$_{110}$** than in **DPCHP-DODE** both at room temperature and in the heating process. Based on which, a possible mechanism for the formation of supramolecular polymer was suggested. In **DPCHP-DODE$_{110}$**, the amide groups of one molecule could form stable intermolecular hydrogen-bonding interactions with amide groups of another molecule, therefore leading to long-range hydrogen-bonding interactions. The intermolecular hydrogen-bonding interactions might be responsible for the occurrence of supramolecular polymer properties after cooling the melting **DPCHP-DODE**. However, supramolecular polymer properties such as thermal properties were not observed in **DPCHP-DODE** due to the lack of intermolecular hydrogen-bonding interactions. Our research has demonstrated that the hydrogen-bonding interactions of

amide groups could become stronger by the substitute effects, which in turn enabled the fabrication of supramolecular polymer from the molecules bearing such groups.

Acknowledgements

This work is supported by the National Natural Science Foundation of China (Nos. 21574074 and 21174079) and National Basic Research Program of China (973 plan, No.2014CB932202).

References

1 L. Brunsveld, B. J. B. Folmer, E. W. Meijer and R. P. Sijbesma, Chem. Rev., 2001, 101, 4071-4098.
2 F. J. M. Hoeben, P. Jonkheijm, E. W. Meijer and A. P. H. J. Schenning, Chem. Rev., 2005, 105, 1491-1546.
3 T. Nakamura, T. Fuke and M. Shibata, Colloid Polym. Sci., 2014, 292, 1261-1268.
4 A. J. P. Teunissen, M. M. L. Nieuwenhuizen, F. Rodriguez-Llansola, A. R. A. Palmans and E. W. Meijer, Macromolecules, 2014, 47, 8429-8436.
5 M. Hayashi, A. Noro and Y. Matsushita, J. Polym. Sci. Pol. Phys., 2014, 52, 755-764.
6 X. M. Zhang, Q. D. Zeng and C. Wang, Rsc Adv., 2013, 3, 11351-11366.
7 B. Roy, P. Bairi and A. K. Nandi, Rsc Adv., 2014, 4, 1708-1734.
8 H. F. Yu, H. Liu and T. Kobayashi, ACS Appl. Mater. Inter., 2011, 3, 1333-1340.
9 Y. Wang, Y. Cao, Y. P. Qiu and L. M. Tang, Macromol. Rapid Comm., 2008, 29, 258-263.
10 A. J. Wilson, Soft Matter, 2007, 3, 409-425.
11 L. Xiao, Y. Xiong, S. Tian, C. He, Q. Su and Z. Wen, Chem. Eng. J. (Amsterdam, Neth.), 2015, 265, 157-163.
12 M. Higuchi, J Mater. Chem. C, 2014, 2, 9331-9341.
13 W. C. Yount, H. Juwarker and S. L. Craig, J. Am. Chem. Soc., 2003, 125, 15302-15303.
14 M. Burnworth, L. M. Tang, J. R. Kumpfer, A. J. Duncan, F. L. Beyer, G. L. Fiore, S. J. Rowan and C. Weder, Nature, 2011, 472, 334-337.
15 C. A. Hunter and J. K. M. Sanders, J. Am. Chem. Soc., 1990, 112, 5525-5534.
16 R. Vaiyapuri, B. W. Greenland, S. J. Rowan, H. M. Colquhoun, J. M. Elliott and W. Hayes, Macromolecules, 2012, 45, 5567-5574.
17 S. Burattini, B. W. Greenland, D. H. Merino, W. G. Weng, J. Seppala, H. M. Colquhoun, W. Hayes, M. E. Mackay, I. W. Hamley and S. J. Rowan, J. Am. Chem. Soc., 2010, 132, 12051-12058.
18 S. Banerjee, R. K. Das and U. Maitra, J. Mater. Chem., 2009, 19, 6649-6687.
19 J. N. Hunt, K. E. Feldman, N. A. Lynd, J. Deek, L. M. Campos, J. M. Spruell, B. M. Hernandez, E. J. Kramer and C. J. Hawker, Adv. Mater., 2011, 23, 2327-2331.
20 H. Chen, X. Ma, S. F. Wu and H. Tian, Angew. Chem. Int. Edit., 2014, 53, 14149-14152.
21 K. M. Huh, T. Ooya, W. K. Lee, S. Sasaki, I. C. Kwon, S. Y. Jeong and N. Yui, Macromolecules, 2001, 34, 8657-8662.
22 X. P. Yang, H. J. Yu, L. Wang, R. B. Tong, M. Akram, Y. S. Chen and X. T. Zhai, Soft Matter, 2015, 11, 1242-1252.
23 P. F. Wei, X. Z. Yan and F. H. Huang, Chem. Soc. Rev., 2015, 44, 815-832.
24 F. Zeng, Y. Shen and C. F. Chen, Soft Matter, 2013, 9, 4875-4882.
25 X. Y. Qiu, Y. H. Yang, L. P. Wang, S. L. Lu, Z. Z. Shao and X. Chen, Rsc Adv., 2011, 1, 282-289.
26 J. X. Ding, L. H. Chen, C. S. Xiao, L. Chen, X. L. Zhuang and X. S. Chen, Chem. Commun., 2014, 50, 11274-11290.
27 S. Y. Dong, L. Y. Gao, J. Z. Chen, G. C. Yu, B. Zheng and F. H. Huang, Polym. Chem.-UK, 2013, 4, 882-886.
28 Y. J. Wang and L. M. Tang, Prog. Chem., 2006, 18, 308-316.
29 J. D. Fox and S. J. Rowan, Macromolecules, 2009, 42, 6823-6835.
30 S. Burattini, B. W. Greenland, W. Hayes, M. E. Mackay, S. J. Rowan and H. M. Colquhoun, Chem Mater, 2011, 23, 6-8.
31 X. X. Chen, M. A. Dam, K. Ono, A. Mal, H. B. Shen, S. R. Nutt, K. Sheran and F. Wudl, Science, 2002, 295, 1698-1702.
32 C. M. Chung, Y. S. Roh, S. Y. Cho and J. G. Kim, Chem. Mater., 2004, 16, 3982-3984.
33 S. Coulibaly, A. Roulin, S. Balog, M. V. Biyani, E. J. Foster, S. J. Rowan, G. L. Fiore and C. Weder, Macromolecules, 2014, 47, 152-160.
34 B. K. Chegeni, A. Kakanejadifard, F. Abedi, R. Kabiri, F. Daneshnia and M. Adeli, Colloid Polym Sci, 2014, 292, 3337-3346.
35 Z. Zhang, Q. Lv, X. Gao, L. Chen, Y. Cao, S. Yu, C. He and X. Chen, ACS Appl. Mater. Inter., 2015, 7, 8404-8411.
36 C. Y. Han, B. Y. Xia, J. Z. Chen, G. C. Yu, Z. B. Zhang, S. Y. Dong, B. J. Hu, Y. H. Yu and M. Xue, Rsc Adv., 2013, 3, 16089-16094.
37 C. He, A. M. Donald, A. C. Griffin, T. Waigh and A. H. Windle, J. Polym. Sci. Pol. Phys., 1998, 36, 1617-1624.
38 A. M. van de Craats, J. M. Warman, A. Fechtenkotter, J. D. Brand, M. A. Harbison and K. Mullen, Adv. Mater., 1999, 11, 1469-1472.
39 L. Gonzalez, L. Y. Yu, S. Hvilsted and A. L. Skov, Rsc Adv., 2014, 4, 36117-36124.
40 S. V. Kolotuchin and S. C. Zimmerman, J. Am. Chem. Soc., 1998, 120, 9092-9093.
41 S. H. M. Sontjens, J. T. Meijer, H. Kooijman, A. L. Spek, M. H. P. van Genderen, R. P. Sijbesma and E. W. Meijer, Org. Lett., 2001, 3, 3887-3889.
42 S. Yagai, T. Iwashima, K. Kishikawa, S. Nakahara, T. Karatsu and A. Kitamura, Chem.-Eur. J., 2006, 12, 3984-3994.
43 R. P. Sijbesma, F. H. Beijer, L. Brunsveld, B. J. B. Folmer, J. H. K. K. Hirschberg, R. F. M. Lange, J. K. L. Lowe and E. W. Meijer, Science, 1997, 278, 1601-1604.
44 B. J. B. Folmer, R. P. Sijbesma, R. M. Versteegen, J. A. J. van der Rijt and E. W. Meijer, Adv. Mater., 2000, 12, 874-878.
45 A. E. Reed, L. A. Curtiss and F. Weinhold, Chem. Rev., 1988, 88, 899-926.
46 R. Parthasarathi, V. Subramanian and N. Sathyamurthy, J Phys. Chem. A, 2006, 110, 3349-3351.
47 A. Mohajeri and F. F. Nobandegani, J. Phys. Chem. A, 2008, 112, 281-295.
48 Q. Z. Li, M. L. An, F. Luan, W. Z. Li, B. A. Gong and J. B. Cheng, J. Phys. Chem. A, 2008, 112, 3985-3990.
49 S. K. Kolev, P. St Petkov, M. A. Rangelov and G. N. Vayssilov, J. Phys. Chem. A, 2011, 115, 14054-14068.
50 P. V. Bernhardt, P. Chin, P. C. Sharpe and D. R. Richardson, Dalton T, 2007, 3232-3244.
51 L. Qiang, J. Y. Zhu, L. M. Tang, Z. H. Dai and K. Chen, Acta Polym. Sin., 2013, 414-418.
52 L. Biczok, T. Berces and H. Inoue, J Phys Chem A, 1999, 103, 3837-3842.
53 C. Heinzmann, S. Coulibaly, A. Roulin, G. L. Fiore and C. Weder, ACS Appl. Mater. Inter., 2014, 6, 4713-4719.
54 J. H. Kim, H. G. Kim, J. C. Lim, K. S. Cho and K. E. Min, J. Appl. Polym. Sci., 2012, 124, 3312-3319.

55 Y. Zhang, H. F. Li, L. J. An and S. C. Jiang, Acta Polym. Sin., 2013, 462-472.
56 D. J. Skrovanek, S. E. Howe, P. C. Painter and M. M. Coleman, Macromolecules, 1985, 18, 1676-1683.
57 S. Sivakova, D. A. Bohnsack, M. E. Mackay, P. Suwanmala and S. J. Rowan, J. Am. Chem. Soc., 2005, 127, 18202-18211.
58 Y. R. Liu, L. S. He, J. Y. Zhang, X. B. Wang and C. Y. Su, Chem. Mater., 2009, 21, 557-563.
59 Y. Maeda, T. Nakamura and I. Ikeda, *Macromolecules*, 2001, **34**, 8246-8251.